Applied Catalysis B: Environmental 307 (2022) 121144

Contents lists available at ScienceDirect

Applied Catalysis B: Environmental

journal homepage: www.elsevier.com/locate/apcatb

Dibenzothiophene-*S*,*S*-dioxide-containing conjugated polymer with hydrogen evolution rate up to 147 mmol g^{-1} h^{-1}

Yuxiang Liu, Jun Wu, Feng Wang *

School of Chemical Engineering and Pharmacy, Wuhan Institute of Technology, Wuhan 430205, PR China

ARTICLE INFO

Keywords:
Donor−acceptor
Dibenzothiophene-*S*
S-dioxide
Thiophene
Hydrogen
Exfoliation

ABSTRACT

Molecular engineering in donor–acceptor conjugated polymers is currently one of the most successful and popular strategy to prepare high performance photocatalysts for hydrogen evolution. In this contribution, we have designed and synthesized two novel conjugated polymers with tailored donor–acceptor structures based on dibenzothiophene-*S*,*S*-dioxide and thiophene derivatives, which exhibited tunable band gaps and adjustable charge separation efficiencies. As a result, PDBTSO-T showed an outstanding hydrogen evolution rate (HER) of 1.47 mmol h^{-1} by DMF exfoliation under UV−vis region with Pt cocatalyst in ascorbic acid aqueous solution at 10 mg level, which is among the top performance for photocatalysis conversion reported so far. Very excitingly, when the photocatalysis tests were subjected to natural sunlight irradiation, an impressive HER of ~27 mL (107 mmol g^{-1} h^{-1}) was achieved after 0.5 h of illumination (12:30 pm – 13:00 pm) on a consistently sunny day under identical reaction conditions.

1. Introduction

Photocatalytic water-splitting is believed to be a promising approach for hydrogen evolution to meet global energy demand in the near future [1–7]. Despite enormous efforts, exploitation of solar light responsive photocatalysts with impressive activity still remains a scientific challenge [4,8]. Organic semiconductors, possessing many advantages compared to inorganic semiconductors, have been regarded as very promising candidates for photocatalysis [9–15]. Since the first report of poly(p-phenylene) as an active material [16], many new classes of organic semiconductors have emerged as novel photocatalysts for hydrogen evolution, such as conjugated microporous polymers [9, 17–19], covalent organic frameworks [20–22], covalent triazine-based frameworks [23–25], and metal–organic frameworks [26,27]. Among the numerous reported organic photocatalysts, conjugated polymers have been widely investigated as easily processable and low-cost materials for solar-driven hydrogen production [10,28,29]. Particularly, the electronic properties of conjugated polymers can be easier tuned by using different organic precursors. With suitable building blocks, some of conjugated polymers demonstrated very impressive energy conversion efficiency for water-splitting [30–32].

To realize a better photocatalytic performance, the development of the polymeric photocatalysts with donor−acceptor structures has demonstrated to be one of the most effective and successful strategies [33–41]. During the photocatalytic process, the inherent dipole character in donor−acceptor conjugation skeleton could touch off intramolecular charge transfer from electron-donating units to electron-deficient units, and the photogenerated electrons might be preferably concentrated into acceptor phase in the excited state, which would efficiently improve the charge carrier separation [42]. Therefore, the photogenerated electrons concentrated acceptor units would help promote the reduction of water. According to this strategy, significant progress on photocatalytic water-splitting by donor−acceptor conjugated polymers using electron deficient dibenzothiophene-*S*,*S*-dioxide (DBTSO) [43–45], triazine [17,24], benzothiadiazole [46,47], or some other heterocycles has been made [28]. Among these acceptor units, DBTSO was widely employed as an attractive accepting unit in polymeric photocatalysts due to its good photochemical stability, well-conjugated structure, high π-electron delocalization [45,48–51]. Several conjugated polymers containing DBTSO units have been demonstrated to exhibit exciting photocatalytic properties with a maximum activity up to 105 mmol g^{-1} h^{-1} in UV−vis region [31,50]. Despite many outstanding advancements being achieved, it is important to rationally tune the chemical structures of DBTSO-based photocatalysts, and to investigate the interplay between the polymer structure and the water-splitting performance. Such insights would provide more

* Corresponding author.
E-mail address: psfwang@wit.edu.cn (F. Wang).

https://doi.org/10.1016/j.apcatb.2022.121144
Received 13 November 2021; Received in revised form 20 January 2022; Accepted 23 January 2022
Available online 29 January 2022

concrete design approaches to prepare high performance DBTSO-based donor−acceptor polymers for photocatalysis. It is well known that thiophene has a six-π-electron five-membered planar structure, which can donate some electron density to the conjugated backbones and promote charge carrier transport [34]. When DBTSO was copolymerized with thiophene, the photogenerated excitons could be efficiently separated, and the separated holes and electrons could greatly accelerate water-splitting reaction.

A natural sunlight photoactive material can provide a more convenient and greener approach for water-splitting, while it needs call for higher photocatalytic efficiency due to the lower solar light intensity. Therefore, there is still little research in this field. Taking these considerations into account, we have rationally designed and synthesized two novel donor−acceptor conjugated polymers, namely, PDBTSO-T and PDBTSO-2 T. The two polymers were composed of DBTSO acceptor units and electron-rich donating segments including thiophene and 2,2′-dithiophene, which increases light harvesting and boosts photogenerated charge carriers. It was found that PDBTSO-T exhibited an extraordinary photocatalytic activity with a hydrogen evolution rate (HER) of 1.47 mmol h^{-1} under UV−vis region with Pt cocatalyst in ascorbic acid (AA) aqueous solution at 10 mg level through DMF exfoliation. More importantly, PDBTSO-T exhibited a comparable photocatalytic activity at a rate of ~ 27 mL (107 mmol g^{-1} h^{-1}) under natural sunlight irradiation on a consistently sunny day. To our best, this efficiency is one of the highest values for polymeric photocatalysts. The influence of the number of thiophene rings on the photocatalytic performance for the resulting polymers were compared and discussed.

2. Experimental

2.1. Synthesis of PDBTSO-T

In a 100 mL flask, 3,7-bis(4,4,5,5-tetramethyl-1,3,2-dioxaborolan-2-yl)dibenzothiophene-*S*,*S*-dioxide (936 mg, 2 mmol), 2,5-dibromothiophene (484 mg, 2 mmol), and $Pd(PPh_3)_4$(0) (20 mg, 0.016 mmol) were dissolved in a mixture of DMF (40 mL) and 2 M Na_2CO_3 (6 mL). The solution was heated to 150 °C with vigorous stirring for 72 h. The precipitated solid was recovered by filtration, and washed with distilled water and methanol to remove impurities. PDBTSO-T was obtained as a brown solid (yield: 82.9%). Anal. calcd for $C_{16}H_8O_2S_2$: C 64.86, H 2.70, O 10.81, S 21.62; found: C 62.21, H 3.04, O 13.47, S 20.70. Pd 0.01 wt% from inductively coupled plasma mass spectrometry (ICP-MS) measurement.

2.2. Synthesis of PDBTSO-2T

PDBTSO-2T was prepared by using the same procedure as that of PDBTSO-T. PDBTSO-2 T was obtained as a dark brown solid (yield: 80.3%). Anal. calcd for $C_{20}H_{10}O_2S_3$: C 63.49, H 2.65, O 8.46, S 25.39; found: C 59.26, H 3.02, O 11.86, S 24.30. Pd 0.014 wt% from ICP-MS measurement.

2.3. Photocatalysis test under simulated light illumination

Typically, the polymer powder (10 mg) was ultrasonically dispersed in 60 mL mixed solvent for 30 min, then 40 mL AA (6.6 g) aqueous solution was added. The varied pH value of the mixture was adjusted by NaOH solution. The Pt cocatalyst was deposited in situ from H_2PtCl_6 (3 wt%) on the surface of polymers. Hydrogen evolution tests were conducted by a Labsolar-6A circulation system (Beijing Perfectlight Technology Co., Ltd). The photocatalytic experiment was irradiated with a Xe light source (300 W) using appropriate filters. The temperature for the mixture solution was maintained at 10 °C by flowing cooling water. The evolved hydrogen was estimated by an online gas chromatograph.

2.4. Photocatalysis test under natural light illumination

The polymer powder (20 mg) was ultrasonically dispersed in 60 mL mixed solvent for 30 min, then 40 mL AA (6.6 g) aqueous solution was added. The pH value of the mixture was adjusted to 4 by NaOH solution. Pt nanoparticles were photo-deposited on the surface of PDBTSO-T from H_2PtCl_6 (3 wt%). The outdoor photocatalysis tests were carried out under solar irradiation on the rooftop of Wuhan Institute of Technology (a longitude of 114.43°E and latitude of 30.46°N). The weather conditions including solar intensity and temperature were periodically recorded from a weather station. The photoreactor comprised a double-walled glass reactor which was connected to an upturned measuring cylinder to estimate the generated hydrogen. The volume of generated hydrogen was measured per half hour on September 3, 2021, in Wuhan, P. R. China.

3. Results and discussion

3.1. Synthesis and characterization

The synthetic route to PDBTSO-T and PDBTSO-2 T are shown in Scheme 1. The two polymers were prepared by Pd-catalyzed Suzuki coupling reaction between diboronic ester and dibromide monomers (see detailed experimental procedure). The resulting polymers show apparent colors ranging from brown to dark brown. The thermal gravimetric analysis revealed that the polymers exhibit good thermal stability under a N_2 atmosphere (Fig. S1).

Their chemical structures were characterized by Fourier transform infrared spectroscopy (FT-IR), solid-state ^{13}C NMR, and X-ray photoelectron spectroscopy (XPS). Two peaks at ca. 1302 and 1160 cm^{-1} are the characteristic stretching vibration bands of sulphone group (O═S═O) (Fig. S2) [32]. At the same time, the stretching vibration band of S–C–S at 706 cm^{-1} was emerged, which is attributed to the incorporation of thiophene units [34]. In solid-state ^{13}C NMR spectra, the characteristic signal at 138 ppm is attributed to the carbon bonding with the sulfone group, and the peaks located at around 133, 125, 122, 117 and 114 ppm can be assigned to aromatic carbons on the DBTSO and thiophene units (Fig. S3). It can be observed that the signal at 120 ppm was shifted gradually to higher field and the peak intensity became gradually stronger from PDBTSO-T to PDBTSO-2 T, owing to the increase of thiophene content in the conjugated framework. In addition, the chemical structures of PDBTSO-T and PDBTSO-2 T were further supported by XPS. The binding energy at ~169.1 and ~167.9 eV could be assigned to S species in sulphone group (Fig. S4) [49]. Two strong peaks at ~163.9 and ~165.0 eV were observed for the polymers, which are related to the S 2p1/2 and S 2p3/2 in thiophene units, respectively. These spectroscopy features suggest that the polymers have been successfully prepared. In addition, elemental analysis of PDBTSO-T and PDBTSO-2T confirms the molecular structures as proposed.

The surface nanomorphology of polymers were examined using scanning electron microscope (SEM). As shown in Fig. S5, PDBTSO-T consisted of similar irregular agglomerated nanoparticles, while PDBTSO-2T exhibited a flake-like structure. Detailed distributions of the elements were probed by energy dispersive X-ray spectrometer mapping. As shown in Fig. S6, the elements C (red), S (blue), and O (green) are mainly distributed in the polymers. Powder X-ray diffraction analysis suggested that PDBTSO-T has an amorphous aggregated structure, while PDBTSO-2T is semi-crystalline (Fig. S7).

3.2. UV–vis absorption and energy band position

The light absorption behaviors are important for the photocatalysts to achieve an impressive light-driven water-splitting performance. Herein, the absorption properties of PDBTSO-T and PDBTSO-2T were studied by UV–vis diffuse reflectance spectra. The two polymers exhibited two distinct absorption peaks, which are commonly observed

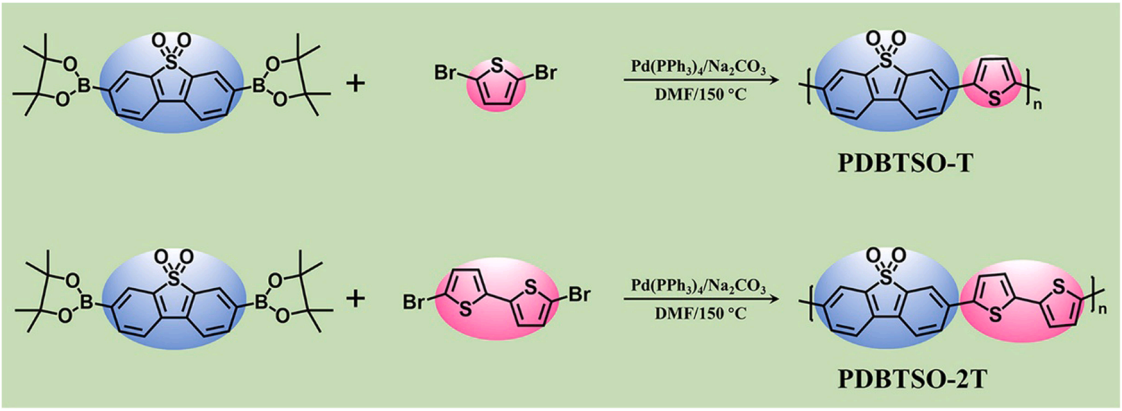

Scheme 1. Synthetic routes to PDBTSO-T and PDBTSO-2T.

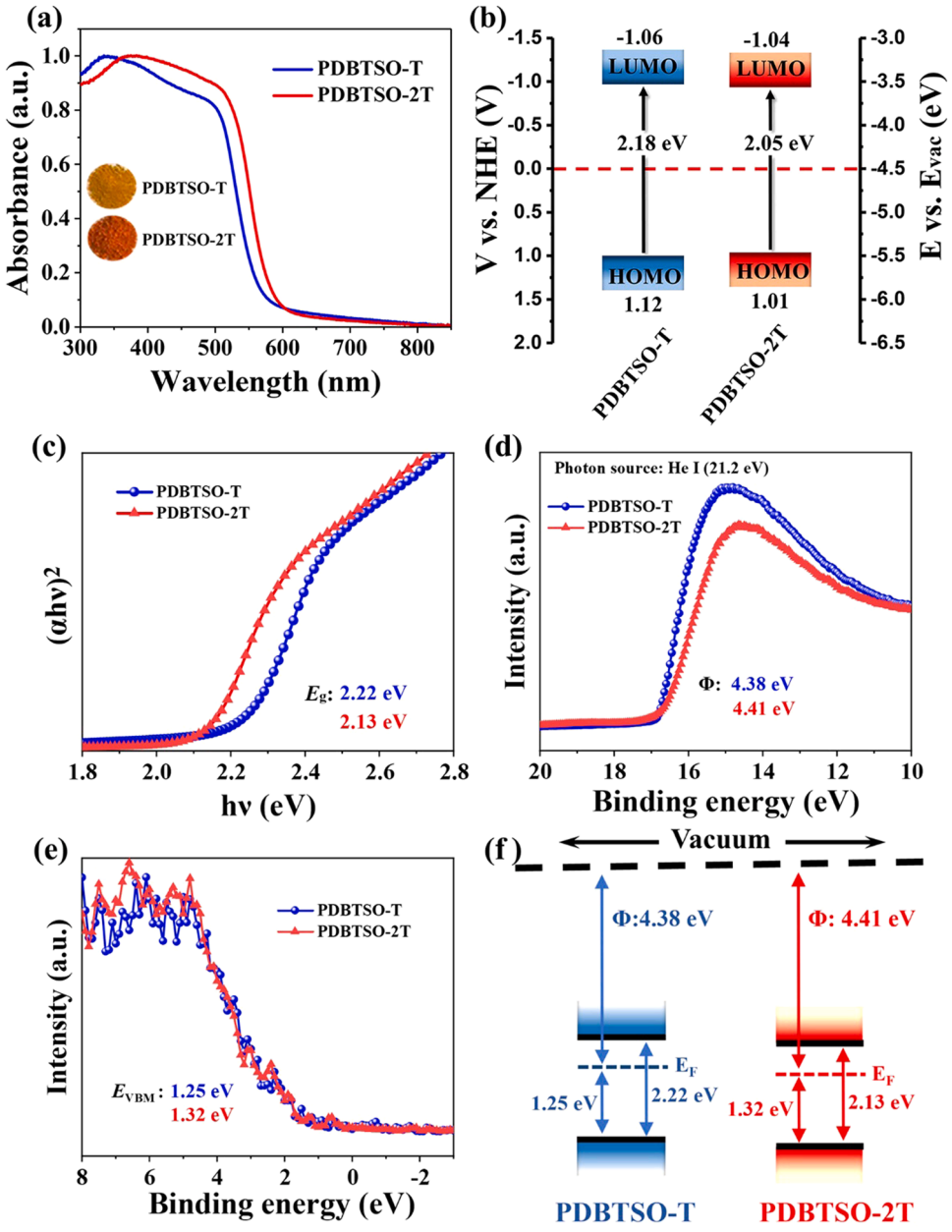

Fig. 1. (a) UV–vis diffuse reflectance spectra, (b) HOMO and LUMO levels, (c) Tauc plots, (d) UPS spectra and (e) XPS valence band spectroscopy of the polymers. (f) Schematic of the band structure position. Inset: Photographs of the polymers.

for the donor−acceptor polymers (Fig. 1a). The strong peaks at short wavelength (388 −428 nm) can be attributed to the π − π*transition of DBTSO segments, while the absorption bands at longer wavelength (558 −589 nm) are from the low-bandgap units [33]. As compared with PDBTSO-T, PDBTSO-2 T exhibited a red-shift of the absorption edge. This is probably due to the extended π − conjugation degree of the low-bandgap units for PDBTSO-2 T than PDBTSO-T. It was noted that the optical bandgap decreases with increasing thiophene content. Cyclic voltammetry (CV) measurement was conducted to study the electrochemical properties of the polymers by using ferrocene/ferrocenium (Fc/Fc^+) reference as an internal standard, which was assigned an absolute energy of − 4.8 eV vs. vacuum level (Fig. S8). Table S1 summarizes electrochemical data for PDBTSO-T and PDBTSO-2 T. The onsets of oxidation/reduction waves of PDBTSO-T and PDBTSO-2 T are calculated to be 1.13/− 1.05 V and 1.02/− 1.03 V, respectively. The HOMO and LUMO levels are − 5.62 and − 3.44 eV for PDBTSO-T and − 5.51 and − 3.46 eV for PDBTSO-2 T according to the empirical formula of $E_{HOMO} = -e(E_{ox} + 4.8 - E_{1/2}^{(Fc/Fc+)})$ (eV) and $E_{LUMO} = -e(E_{re} + 4.8 - E_{1/2}^{(Fc/Fc+)})$ (eV), respectively. Thus, the electrochemical band gaps are 2.18 eV for PDBTSO-T and 2.05 eV for PDBTSO-2 T (Fig. 1b). The LUMO positions of the polymers are higher than the water reduction potential, suggesting that the thermodynamical force can drive water-splitting half reaction [5].

Furthermore, the Mott-Schottky plots were used to reveal the energy band of the two polymers. As shown in Fig. S9, PDBTSO-T and PDBTSO-2 T are typical n-type organic semiconductors because of the positive slopes. The flat-band potentials are estimated to be –1.21 and −1.17 V vs. standard calomel electrode (SCE) for PDBTSO-T and PDBTSO-2 T, respectively. The conduction band (CB) potential is roughly equal to the flat-band potential for a n-type semiconductor [52]. Thus, the CB of PDBTSO-T and PDBTSO-2 T are calculated to be ca. − 0.97 and −0.93 V vs. normalized hydrogen electrode (NHE), respectively. The optical bandgaps are estimated to be 2.22 eV for PDBTSO-T and 2.13 eV for PDBTSO-2 T from the Tauc plots (Fig. 1c). The valence band (VB) of PDBTSO-T and PDBTSO-2 T are calculated to be ca. 1.25 and 1.20 V, respectively.

To further investigate the band position of the two polymers, the work function (Φ) and VB were calculated using UPS and XPS measurements, respectively. As shown in Fig. S10, the secondary edges (E_{SE}) for PDBTSO-T and PDBTSO-2 T were determined to be 16.82 and 16.79 eV, respectively. According to the empirical formula, the corresponding Φ were calculated to be 4.38 eV for PDBTSO-T and 4.41 eV for PDBTSO-2T (Fig. 1d) [53]. Based on XPS spectroscopy, the calculated VB maximum position (E_{VBM}) vs. Fermi level of PDBTSO-T and PDBTSO-2T are 1.25 and 1.32 eV, respectively (Fig. 1e). A schematic diagram of energy band structures of the two polymers is displayed in Fig. 1f from UPS, XPS and UV–vis absorption analysis, which is moderately consistent with the results from CV and Mott-Schottky measurements.

3.3. Photocatalysis tests

Photocatalytic hydrogen production (PHP) of the polymers was investigated using 10 mg sample in an aqueous solution. Distinct kinds of sacrificial agent exhibited different effect on the photocatalytic system. Accordingly, choosing an effective and suitable sacrificial agent becomes so important for the enhancement of hydrogen evolution activity [28]. To fully investigate photocatalytic water-splitting performance of the two polymers, we selected the four widely used sacrificial agents including methanol, methanol/triethylamine (TEA), triethanolamine (TEOA), and AA. No additional precious metal cocatalyst (e.g., Pt) was used for the initial photocatalysis test. In the case of TEOA addition, the bare photocatalysts exhibited a molecular structure dependent HER in the test period of 4 h. PDBTSO-T and PDBTSO-2 T showed moderate rates of 47 and 44 μmol h^{-1}, respectively (Fig. 2 and Table S2). In addition, the photocatalytic HERs were further tested by using other two sacrificial agents of methanol, methanol/TEA. Unexpectedly, the two polymers exhibited lower photocatalytic performance under the identical conditions. The poor photocatalytic activity of the polymers with three sacrificial agents mentioned above might be mainly ascribed to their low LUMO energy levels, which are quite close to the H_2O/H_2 redox potential in aqueous solution, providing the limited thermodynamic driving force for proton reduction during the photoreactions (Fig. 3a).

However, the photocatalytic activity was remarkably increased with AA as the electron donor under the identical conditions, as shown in Fig. 2. The pH values were measured to be 4.0 and 10.87 for AA/H_2O and $TEOA/H_2O$ aqueous solutions, respectively. The corresponding reduction potentials of AA/H_2O and $TEOA/H_2O$ were estimated to − 0.236 V and − 0.641 V (vs. NHE), respectively (Fig. 3a). The AA aqueous solution exhibited more positive H^+/H_2 reduction than $TEOA/H_2O$ under the same condition, indicating a higher driving force between the water reduction potential and the photocatalyst with lower LUMO energy level. Therefore, the photocatalytic activities of PDBTSO-T and PDBTSO-2 T in AA/H_2O were remarkably increased. As shown in Fig. 2, among the bare photocatalysts, PDBTSO-T shows better photocatalytic activity with a rate of 508 μmol h^{-1} in the test period of 4 h at 10 mg level.

Recently, some reports mentioned that the residual Pd in the polymer matrix would act as a cocatalyst, which might promote hydrogen evolution [54]. However, no significant Pd signal could be observed for the prepared polymers by energy-dispersive X-ray spectroscopy measurements because of the low Pd concentration (Fig. S11). In addition, ICP-MS revealed that the residual Pd contents vary between 0.01% and

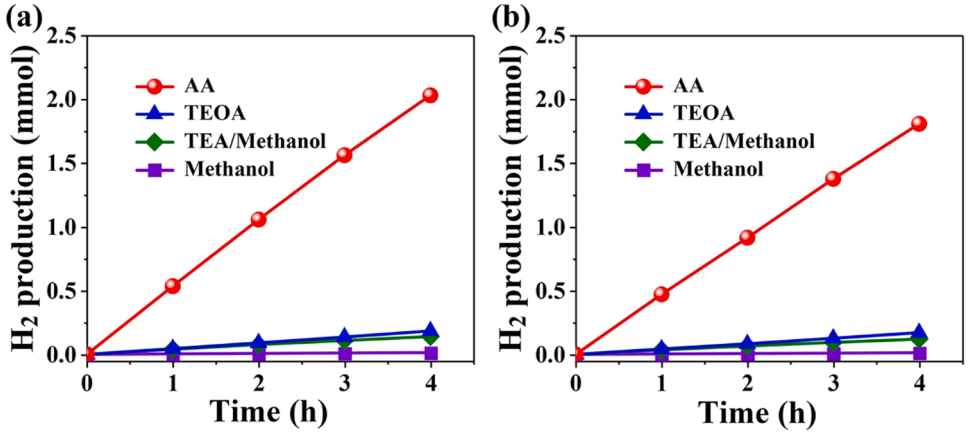

Fig. 2. HERs of (a) PDBTSO-T and (b) PDBTSO-2T. Reaction condition: 10 mg polymer, 100 mL AA (0.4 M) aqueous solution, pH = 4.0.

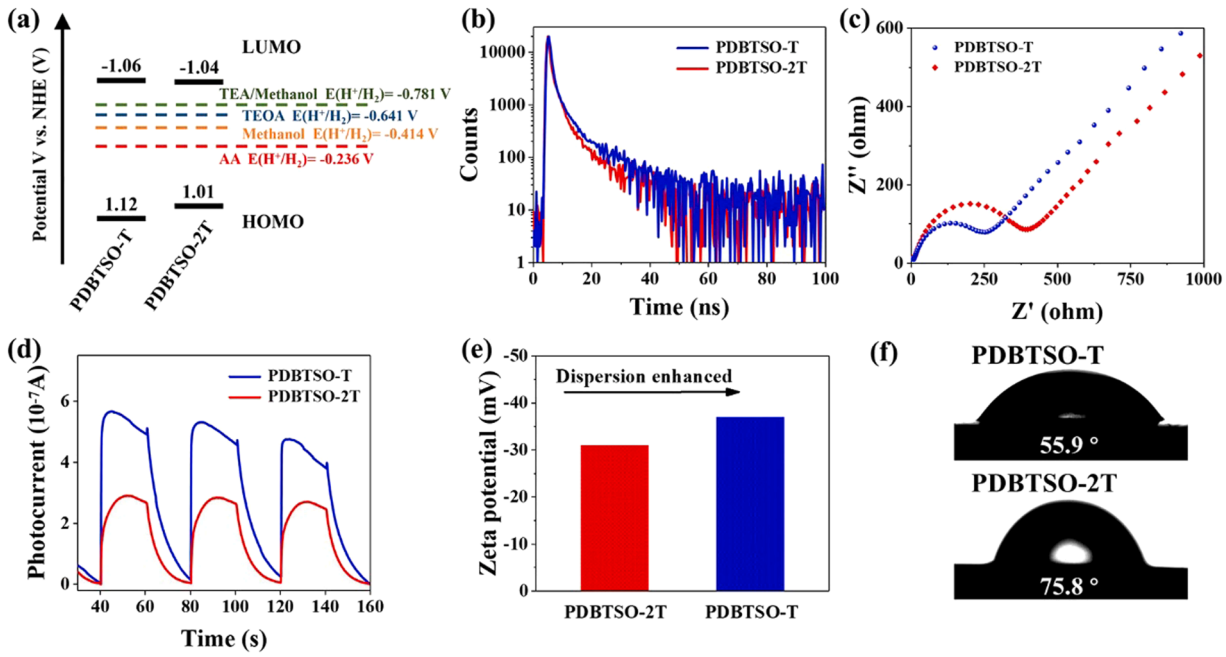

Fig. 3. (a) Schematic energy diagram, (b) time-resolved PL spectra, (c) electrochemical impedance spectroscopy, (d) transient photocurrent, (e) zeta potential, and (f) water contact angles of PDBTSO-T and PDBTSO-2T.

0.02%. Therefore, it might suggest that the trace Pd cocatalyst has a negligible effect on the activity of PDBTSO-T and PDBTSO-2 T.

It is well known that light responsive region of the photocatalyst have significant effects on their hydrogen production activity. If the active material absorbed more light, it would produce more photoexcited electrons, resulting in better water-splitting performance. However, the hydrogen production efficiency follows the order of PDBTSO-T > PDBTSO-2 T in this study, which suggest that spectral absorption might be not necessarily key factor for their photocatalytic activity. In other words, it is difficult to elucidate the different photocatalytic activity among PDBTSO-T and PDBTSO-2 T based on the differences of their absorption regions, since there seems no obvious tendency to be obtained. Therefore, the differences in photocatalytic activity should be caused by differences of electronic configuration, excited state lifetime, charge generation and separation efficiency, charge mobility, wettability and so on [1].

To investigate the pull–push interaction in the conjugated donor–acceptor structure on the photocatalytic activity, we conducted the photophysical spectroscopy tests. Time-resolved PL measurement was carried out to elucidate the charge transfer efficiency, and the estimated values of lifetimes are shown in Table S3. Generally, all the polymers have high photogenerated charge transfer efficiencies due to the strong pull–push interaction brought about donor−acceptor structures [34]. By comparison, the excited-state lifetime of PDBTSO-T is 3.19 ns, obvious longer than that of PDBTSO-2 T (2.48 ns), which closely correlates with the better photocatalytic activity obtained for PDBTSO-T (Fig. 3b). The charge separation and transfer properties of PDBTSO-T and PDBTSO-2 T were further studied by a combined test of electrochemical impedance spectroscopy and photocurrent. PDBTSO-T displayed the smallest arc radius in the Nyquist plot (Fig. 3c), suggesting that the interface of PDBTSO-T exhibit the best charge migration ability. Moreover, PDBTSO-T showed the higher photocurrent response than PDBTSO-2 T under light illumination (Fig. 3d). Overall, the photocatalytic activity of polymers is in the order of PDBTSO-T > PDBTSO-2 T, which is in good agreement with the charge separation efficiency as mentioned above.

Zeta potential was carried out to evaluate the stability of the polymers in suspension (Fig. 3e). The zeta potential of PDBTSO-T was estimated to be − 36 mV, suggesting a higher stability of its nanoparticles when compared with that of PDBTSO-2 T nanoparticles (−32 mV). When nanoparticles have sufficiently large zeta potential values, they would repel each other to against their agglomeration and provide more reaction sites, which is beneficial for PHP. Therefore, the difference in the PHP might be partly ascribed to the variations in zeta potential. In addition, the surface hydrophilicity of the polymers was measured using water contact angle (Fig. 3f). Their wetting behavior could be arranged in the following sequence: PDBTSO-T (55.9°) < PDBTSO-2 T (75.8°), suggesting better hydrophilic property on the polymer PDBTSO-T, which will increase photocatalyst dispersibility in aqueous environment and subsequent can be favorable for proton reduction [48].

3.4. Mechanism study

We next calculated the frontier orbital distribution of the molecular fragments as models to reveal the intrinsic donor–acceptor property in the polymers. The density functional theory (DFT) simulation demonstrated that the basic repeating units express an obvious donor–acceptor characteristic containing the electron-donating thiophene and the electron-withdrawing DBTSO moieties and separated HOMO and LUMO orbits (Fig. 4a). In the HOMO state, the photogenerated electron density mainly populates on the thiophene unit. While in the LUMO state, the electron density is largely localized DBTSO moiety. The separated HOMO and LUMO orbits would promote the migration of photogenerated charge, which facilitates the water-splitting reaction [43].

It is well known that the oxygen atom in the sulphonyl group is the key reaction site for proton reduction [33]. In order to theoretical investigate the effect of electronic properties on their activities, the Mulliken atomic charges of the fragmental structures was employed. As shown in Fig. 4b, the oxygen atom in the sulphonyl group possesses the largest concentrated negative Mulliken charge in all cases, suggesting the strong ability in photogenerated electron concentrating, and which would possess a large driving force for hydrogen evolution reaction [43]. This implies that electron-concentrating ability account for the obtained impressive activity in the two polymers. In other words, the atomic charge screening in PDBTSO-T and PDBTSO-2 T demonstrates

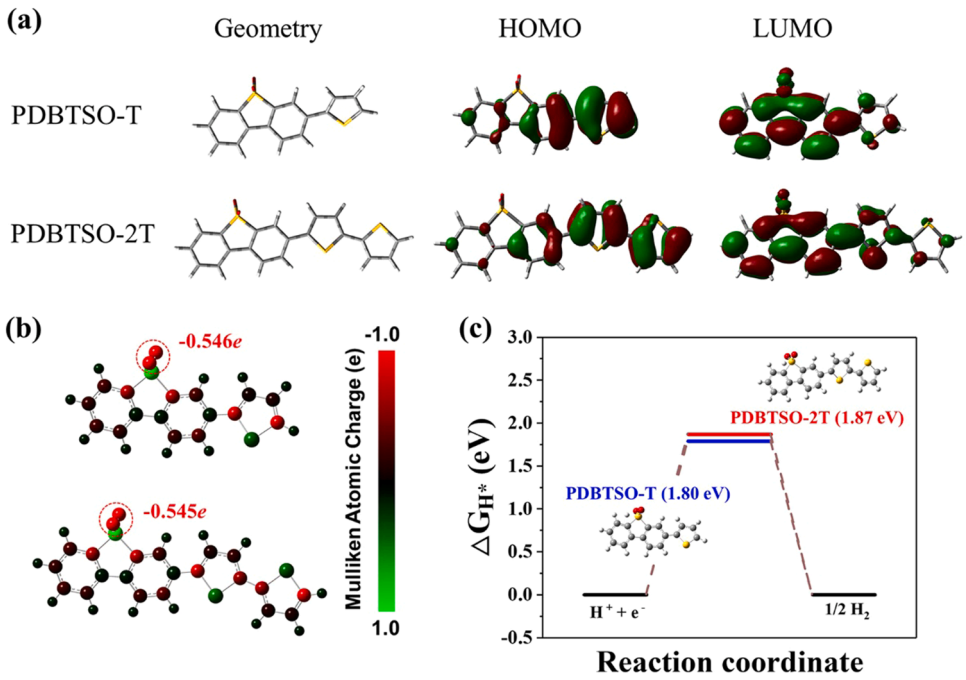

Fig. 4. (a) DFT calculated frontier orbitals for molecular models of PDBTSO-T and PDBTSO-2T. (b) Simulated Mulliken atomic charges of the repeat units of the polymers. (c) The calculated hydrogen-binding free energy at the oxygen site on DBTSO.

the oxygen atom in the sulphonyl group to be reactive site. Moreover, hydrogen-binding free energy (ΔG_{H^*}) was carried out to simulate the photocatalytic potential of the active site in the polymers. Ideally, an active site might be absorbed hydrogen neither too strongly nor too weakly and generally had a ΔG_{H^*} of 0 eV [43,55]. It is well known that Pt is one of the most efficient cocatalyst for PHP because its ΔG_{H^*} of value is closer to 0 eV [43,55]. In this work, the ΔG_{H^*} of sulphonyl oxygen site in PDBTSO-T and PDBTSO-2 T were calculated to be 1.80 and 1.87 eV (Fig. 4c), respectively. It was observed that PDBTSO-T exhibited the lower ΔG_{H^*} of the oxygen site as compared to PDBTSO-2 T. The oxygen atom in the sulphonyl group is used as the active site for hydrogen production, as mentioned above. The oxygen with lone-pair electrons can bond with empty orbital of H to become activated H, and subsequently react with another H to generate hydrogen. Therefore, it is reasonable that PDBTSO-2 T with more thiophene units in the skeleton may weaken the charge density of sulphonyl oxygen and has a negative impact on the H-adsorption–reduction process. These results suggested that the outstanding photocatalytic activity of PDBTSO-T is derived from lower ΔG_{H^*} in the two polymers owing to the suitable electron configuration, which avoid the big barrier for hydrogen formation and release.

3.5. *Effect of cosolvents and pH values on photocatalytic activity*

In addition to the rational design polymeric photocatalysts, activity might be enhanced by the optimization of nanomorphology of photocatalyst [30,50]. Four aprotic polar solvents including NMP, DMI, DMSO, DMF, were employed as additives in the reaction medium. Due to their high surface energy, these four cosolvents can be regarded as suitable reagents for the liquid exfoliation of polymeric photocatalysts [30,31]. For the photocatalysis tests, PDBTSO-T (10 mg) was initially dispersed in 60 mL of cosolvent aqueous solution for 30 min, then 40 mL AA aqueous solution was added. As shown in Fig. 5a, all the PHPs of PDBTSO-T/cosolvent systems were better than that of raw PDBTSO-T without cosolvents in AA solution. The HERs of PDBTSO-T/cosolvent for DMF, DMSO, DMI, and NMP were 86.2, 61.7, 60.3, and 59.6 mmol g^{-1} h^{-1}, respectively.

Contact angle tests were conducted to investigate the surface hydrophilicity of PDBTSO-T toward cosolvents. As shown in Fig. S12, the contact angle of PDBTSO-T is remarkably decreased in the presence of

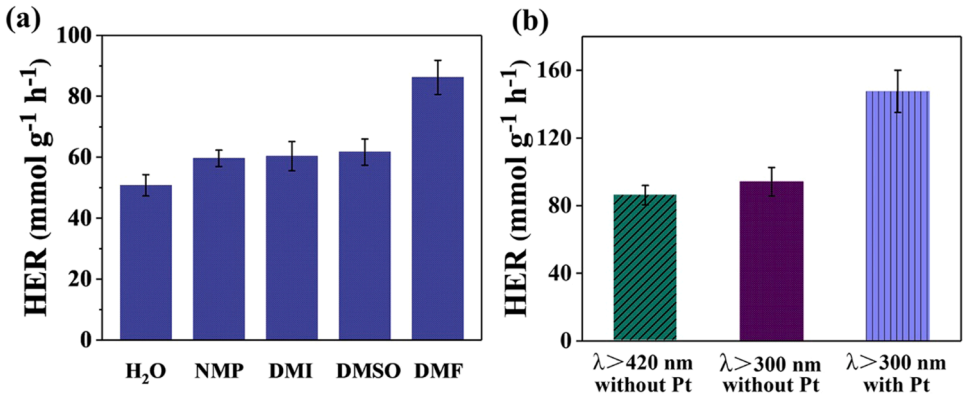

Fig. 5. (a) HER of PDBTSO-T dispersed in varied cosolvents under visible light. (b) HER of PDBTSO-T under various experimental conditions. Experimental conditions: 10 mg sample; 100 mL aqueous solution; under UV–vis or visible light irradiation; with or without Pt cocatalyst.

organic cosolvents, which suggested that the surface of PDBTSO-T became more hydrophilic in the mixed solvent. PDBTSO-T almost reached full-wetting with a contact angle of ~7.3° in DMF aqueous solution, which might be beneficial for water absorption and thus increase proton reduction for hydrogen production. Dynamic light scattering (DLS) technique was applied to compare the particle diameter of the solvent-exfoliated particles to that of the bulk sample. As shown in Fig. 6a, PDBTSO-T dispersed in AA aqueous solution consist of irregular agglomerated large particles with size ranging from 400 to 800 nm. With the addition of aprotic polar cosolvents, the particle size of PDBTSO-T was obviously reduced (Fig. 6b–e). It is noted that PDBTSO-T exhibited a more obvious nanoscale fraction with particle sizes between 200 and 400 nm with the aid of DMF. Confocal laser scanning microscopy (CLSM) measurement was further investigated the exfoliation effect by the aprotic polar solvents on the particle size of PDBTSO-T. As shown in Fig. 6f–j, the particle sizes estimated by the CLSM images were well consist with the results from DLS measurement. From the enlarged inset image (Fig. 6j), PDBTSO-T almost reaches the minimum particle size at around 180 nm in DMF/H_2O, which accounts for its highest photocatalytic activity among these four solvents. These results demonstrated that the cosolvent exfoliation of PDBTSO-T by NMP, DMI, DMSO, and DMF can be beneficial for enhancement of PHP efficiency. Once the bulk PDBTSO-T was exfoliated into nanoparticles, the buried active sites within photocatalyst could be open to reaction medium, which would promote interfacial PHP reaction [50]. In addition, it is well known that exciton diffusion lengths in polymeric photocatalysts are usually limited as short as 5 − 20 nm. The exfoliated PDBTSO-T might remarkably shorten migration distance of the excited excitons, which will drive the corresponding photocatalysis process more efficient [30].

In addition to the important factor of organic cosolvents, the pH values of the aqueous solution might be another key point for determination of their photocatalytic performance. The pH value of an original PDBTSO-T/AA/DMF/H_2O solution is ca. 2.8 without NaOH treatment. Moreover, a series of the aqueous solution with other pH values including 4.0, 5.0, 6.0, and 7.0 with pH adjustment were prepared and used for hydrogen production reaction. As shown in Fig. S13, PDBTSO-T showed a moderate HER of 62.1 mmol h^{-1} g^{-1} with pH value of 7.0. The photocatalytic activity was progressively increased when the pH value was decreased from 7.0 to 4.0, and the resulting photocatalysis system with the optimum acidity of pH = 4.0 exhibited the highest HER of 86.2 mmol h^{-1} g^{-1}. This result suggested that the low pH value was beneficial for proton reduction in this reaction condition. However, the HER of PDBTSO-T became decreased in original solution of AA/DMF/H_2O (pH = 2.8), which suggested that higher acidity in the present system might adversely affects hydrogen evolution. It is inferred that oxidative half-reaction is suppressed at lower pH value. Another observation is that PDBTSO-T exhibited negligible activity at different pH values in DMF/H_2O in the absence of AA (Fig. S13), which further emphasized the importance of a sacrificial reagent for avoiding the recombination of charge carriers and thus enhanced the photocatalytic performance.

3.6. Full-arc irradiation and Pt cocatalyst on PHP

To investigate the correlation between PHP performance and light absorption, we carried out the photocatalysis test for the exfoliated PDBTSO-T in AA/DMF/H_2O solution under full-arc irradiation. It was observed that PDBTSO-T exhibited a HER of 94.1 mmol g^{-1} h^{-1}, which was only slightly more active than that in the visible region (Fig. 5b). These results implied that ultraviolet light shows little contribution for hydrogen production reaction of PDBTSO-T.

Most of conjugated polymers cannot obtain attractive PHP performance without cocatalysts, whereas our results indicated that PDBTSO-T might be employed as high-performance metal-free photocatalyst for PHP [28]. It is well-known that Pt has been considered as the most suitable effective cocatalysts in PHP because of its largest work function and most effective proton reduction for hydrogen production. To further investigate the effect of metal cocatalysts, we carried out the PHP test by using PDBTSO-T with Pt cocatalyst from precursor H_2PtCl_6 under UV−vis light irradiation in AA/DMF/H_2O solution. As shown in Fig. 5b, the HER of PDBTSO-T could be further boosted by Pt cocatalyst and reached up to 147 mmol g^{-1} h^{-1}, which highlight the importance of photogenerated electron transport from PDBTSO-T to the deposited Pt cocatalysts for the enhancement of PHP performance. The impressive HER of 1.47 mmol h^{-1} for 10 mg PDBTSO-T is much higher than most of polymeric photocatalysts except for CP-St [30]. In fact, the obtained photocatalytic activity represents the state-of-the-art of conjugated polymer-based photocatalysts under the identical conditions.

To confirm the reliability of the result mentioned above, a control photocatalysis experiment was conducted on a home-made setup with PDBTSO-T under the identical conditions. After being UV−vis light illumination for 1 h, 10 mg PDBTSO-T dispersed in AA/DMF/H_2O produced 30 mL hydrogen (1.19 mmol, 1.19 mmol h^{-1}/10 mg), which is comparable to the value of obtained from gas chromatograph measurement (see the Supplementary video 1).

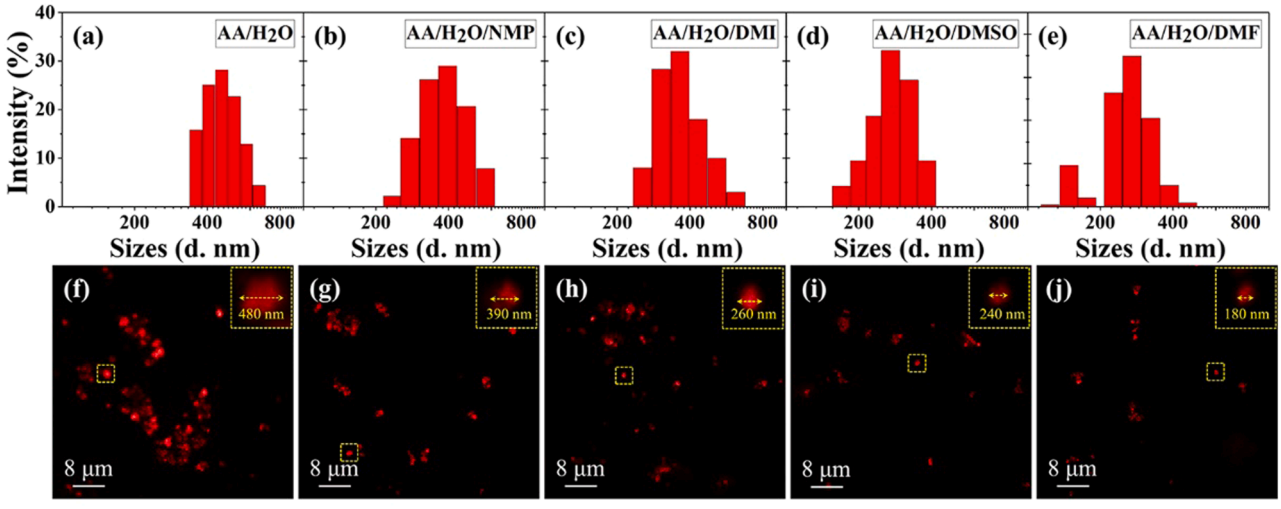

Fig. 6. (a–e) Particle size measurement of PDBTSO-T. (f–j) CLSM images of the nanostructures of PDBTSO-T. Scale bar: 8 μm. Inset: Expansion of nanoparticle pointed with white arrow.

Supplementary material related to this article can be found online at doi:10.1016/j.apcatb.2022.121144.

3.7. Photocatalytic stability measurement

Considering the better photocatalytic efficiency of PDBTSO-T, we prepared the other three batches of the sample under same experimental conditions in order to study the reproducibility of photocatalytic activity. As shown in Fig. 7a, the water-splitting performance did not exhibit significant changes for PDBTSO-T from different batches in the presence of AA and Pt cocatalyst under UV−vis light irradiation, revealing an excellent photocatalytic repeatability. In addition, PDBTSO-T also represents the stable photocatalytic performance without loss in activity after continuous hydrogen production test for 20 h (Fig. 7b). The chemical structures of recycled sample did not show any apparent change in the TEM, FT-IR, XRD, SEM, and UV−vis absorption spectrum (Figs. S14–S18), demonstrating that the photocatalyst PDBTSO-T had structural stability.

3.8. Photocatalysis test under natural sunlight irradiation

A remarkable advantage of PDBTSO-T is that it is highly efficient for PHP. Therefore, the photocatalysis tests employed under natural sunlight irradiation would pave the road towards the practical hydrogen evolution [3]. The PHP reactions were conducted in a Pyrex reactor under solar irradiation on the rooftop of Wuhan Institute of Technology (Fig. 8a). The photoreactor was filled with the AA/DMF aqueous solution (100 mL) in the presence of 20 mg PDBTSO-T powder. In addition, sunlight intensity was measured by using a PL-MW2000 photoradiometer. Supplementary video 2 illustrated collection of moist hydrogen gas generated in the Pyrex reactor under natural sunlight between 10:00 am and 18:00 pm in a consecutive sunny day on 3rd September 2021. Plentiful bubbles of the generated hydrogen can be clearly observed during water-splitting reaction. The peak HER was achieved from 12:30–13:00 pm at the sunlight intensity of 63.4 mW cm^{-2}, and 27 mL hydrogen gas was obtained by 20 mg PDBTSO-T in 0.5 h (Table S4), corresponding to a rate of 107 mmol g^{-1} h^{-1}, which is comparable to the value of 147 mmol g^{-1} h^{-1} measured by an indoor photocatalysis test in the UV−vis region (Fig. 8b). The HER value might vary by time, and other ambient conditions under natural sunlight. Given the durability of the PDBTSO-T-based system, we attributed the decreased HER to the weather condition changes that could reduce the solar irradiation power [3]. Note that the photocatalyst PDBTSO-T is highly active even under a low sunlight intensity of 23.7 mW cm^{-2} at 18:00 pm, suggesting the impressive practicability of the PDBTSO-T-based system (Fig. 8b).

Supplementary material related to this article can be found online at doi:10.1016/j.apcatb.2022.121144.

3.9. The proposed photocatalytic hydrogen evolution mechanism

Based on the above results, the photocatalytic reaction mechanism is shown in Fig. 9. PDBTSO-T exhibited an obvious donor–accepter character and separated HOMO and LUMO orbits. During photoexcitation, the photogenerated electrons would migrate from the HOMO orbits to LUMO orbits of PDBTSO-T. The strong pull–push interaction might accelerate photogenerated electrons transfer from the donor to the accepter. Some excited electrons would further transfer from the LUMO orbits to Pt nanoparticles because of the positive Schottky barrier at PDBTSO-T/Pt interface, which enhance the electron transfer more efficient to facilitate proton reduction reaction. Meanwhile, the photogenerated holes in the HOMO orbits were consumed by sacrificial reagent AA, which reduces the recombination of the electron-hole pairs and promotes photocatalytic water-splitting reaction.

4. Conclusions

In conclusion, we have synthesized two novel donor−acceptor conjugated polymers containing DBTSO electron deficient units and different electron rich units through Suzuki coupling polymerization. Benefiting from the intramolecular charge separation feature among DBTSO and thiophene, strong light harvesting property of thiophene unit, and the hydrophilic nature of DBTSO moiety, the raw PDBTSO-T shows an impressive PHP performance of 50.8 mmol g^{-1} h^{-1} using AA as sacrificial reagent in the visible region. The cosolvent-assisted strategy was applied to increase the PHP activity of DBTSO-based polymers by introducing aprotic solvents. The results suggested that DMF was the best suitable cosolvent to accelerate hydrogen production performance. Therefore, 10 mg photocatalyst PDBTSO-T can generate ~30 mL hydrogen (1.19 mmol) by DMF-exfoliation for 1 h with a continuous full-arc irradiation in AA aqueous solution, which is the highest efficiency reported so far except for CP-St. More importantly, PDBTSO-T exhibited a comparable photocatalytic activity at a rate of ~ 27 mL (107 mmol g^{-1} h^{-1}) under natural sunlight irradiation on a consistently sunny day. To our best, only few works has been carried out on the PHP of conjugated polymers under natural sunlight irradiation. The excellent photocatalytic activity of PDBTSO-T under both simulated and natural sunlight conditions can be mainly attributed to conjugated donor−acceptor structure, strong light absorption properties, exfoliation effect by DMF cosolvent. This study not only highlights the important role of thiophene units on the high-performance of DBTSO-containing donor−acceptor polymers but also gives guidelines for the design of efficient photocatalysts for water-splitting under natural sunlight irradiation in the future.

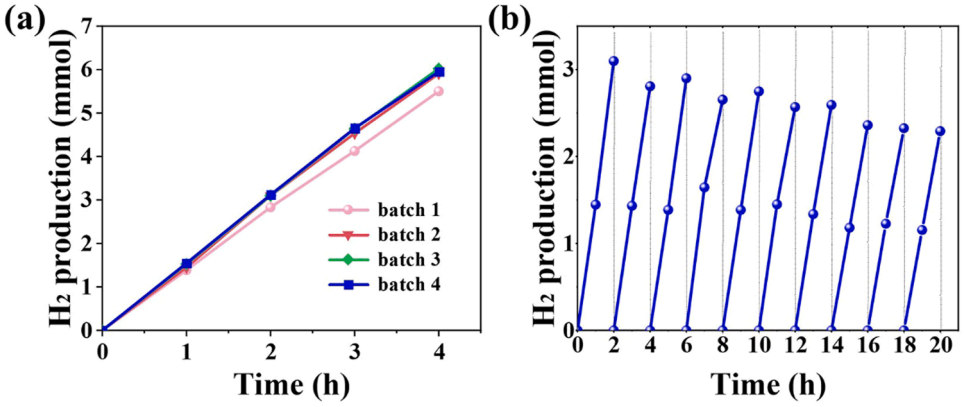

Fig. 7. (a) Hydrogen generation of PDBTSO-T from different batches. (b) Stability test of PDBTSO-T.

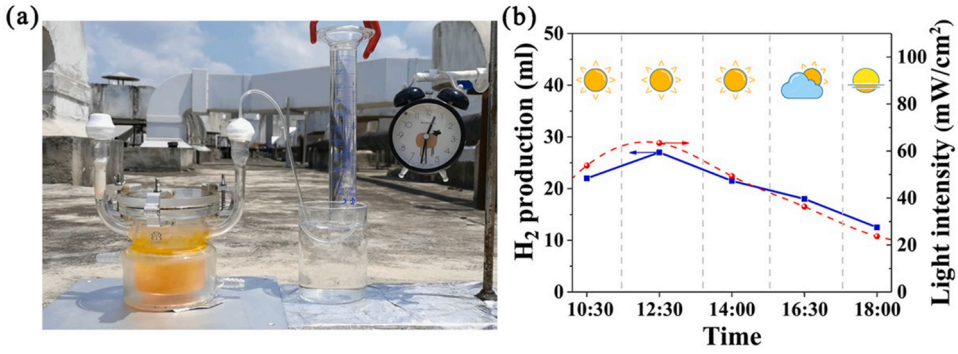

Fig. 8. (a) A photographic image of the photoreactor set-up connected to a hydrogen gas collection vessel. Experimental conditions: 20 mg PDBTSO-T; 100 mL AA/DMF aqueous solution; Pt cocatalyst. (b) PHP performance was acquired on a consistently sunny day (September 3, 2021) under various light intensities at Wuhan Institute of Technology.

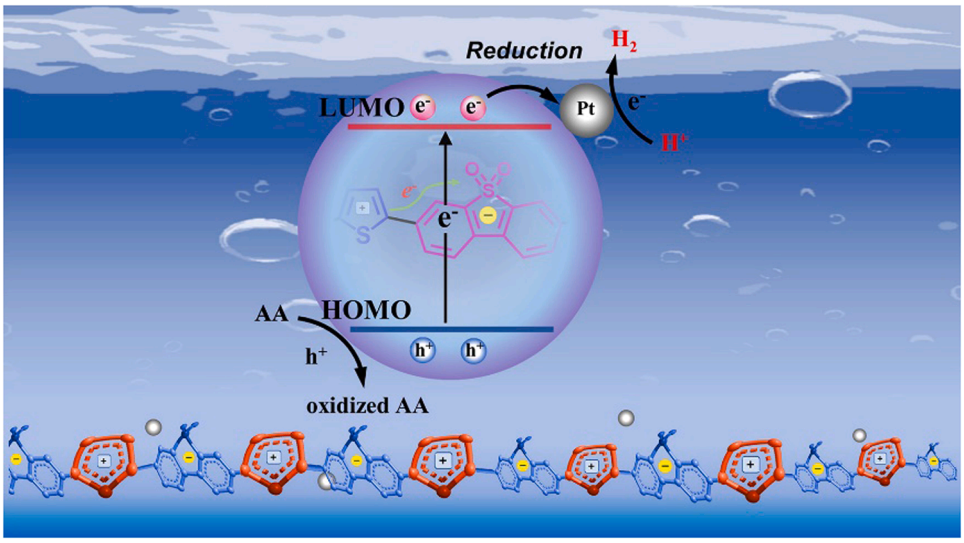

Fig. 9. Proposed mechanism for photocatalytic hydrogen production.

CRediT authorship contribution statement

Yuxiang Liu: Investigation, Methodology, Formal analysis, Data curation, Resources. **Jun Wu**: Data curation. **Feng Wang**: Supervision, Writing – review & editing.

Declaration of Competing Interest

The authors declare that they have no known competing financial interests or personal relationships that could have appeared to influence the work reported in this paper.

Acknowledgements

This work was supported by Educational Commission of Hubei Province of China (D20181505), the Opening Project of Key Laboratory of Optoelectronic Chemical Materials and Devices of Ministry of Education, Jianghan University (JDGD-202003).

Appendix A. Supporting information

Supplementary data associated with this article can be found in the online version at doi:10.1016/j.apcatb.2022.121144.

References

[1] Y.O. Wang, A. Vogel, M. Sachs, R.S. Sprick, L. Wilbraham, S.J.A. Moniz, R. Godin, M.A. Zwijnenburg, J.R. Durrant, A.I. Cooper, J.W. Tang, Current understanding and challenges of solar-driven hydrogen generation using polymeric photocatalysts, Nat. Energy 4 (2019) 746–760, https://doi.org/10.1038/s41560-020-0651-4.

[2] J.H. Kim, D. Hansora, P. Sharma, J.W. Jang, J.S. Lee, Toward practical solar hydrogen production–an artificial photosynthetic leaf-to-farm challenge, Chem. Soc. Rev. 48 (2019) 1908–1971, https://doi.org/10.1039/C8CS00699G.

[3] H. Nishiyama, T. Yamada, M. Nakabayashi, Y. Maehara, M. Yamaguchi, Y. Kuromiya, Y. Nagatsuma, H. Tokudome, S. Akiyama, T. Watanabe, R. Narushima, S. Okunaka, N. Shibata, T. Takata, T. Hisatomi, K. Domen, Photocatalytic solar hydrogen production from water on a 100 m^2-scale, Nature 598 (2021) 304–307, https://doi.org/10.1038/s41586-021-03907-3.

[4] Z. Wang, C. Li, K. Domen, Recent developments in heterogeneous photocatalysts for solar-driven overall water splitting, Chem. Soc. Rev. 48 (2019) 2109–2125, https://doi.org/10.1039/C8CS00542G.

[5] X.B. Chen, S.H. Shen, L.J. Guo, S.S. Mao, Semiconductor-based photocatalytic hydrogen generation, Chem. Rev. 110 (2010) 6503–6570, https://doi.org/10.1021/cr1001645.

[6] Q. Wang, K. Domen, Particulate photocatalysts for light-driven water splitting: mechanisms, challenges, and design strategies, Chem. Rev. 120 (2020) 919–985, https://doi.org/10.1021/acs.chemrev.9b00201.

[7] J.X. Low, J.G. Yu, M. Jaroniec, S. Wageh, A.A. Al-Ghamdi, Heterojunction photocatalysts, Adv. Mater. 29 (2017), 1601694, https://doi.org/10.1002/adma.201601694.

[8] N. Serpone, A.V. Emeline, V.K. Ryabchuk, V.N. Kuznetsov, Y.M. Artem'ev, S. Horikoshi, Why do hydrogen and oxygen yields from semiconductor-based photocatalyzed water splitting remain disappointingly low? Intrinsic and extrinsic factors impacting surface redox reactions, ACS Energy Lett. 1 (2016) 931–948, https://doi.org/10.1021/acsenergylett.6b00391.

[9] N. Chaoui, M. Trunk, R. Dawson, J. Schmidt, A. Thomas, Trends and challenges for microporous polymers, Chem. Soc. Rev. 46 (2017) 3302–3321, https://doi.org/10.1039/C7CS00071E.

[10] C.H. Dai, B. Liu, Conjugated polymers for visible-light-driven photocatalysis, Energy Environ. Sci. 13 (2020) 24–52, https://doi.org/10.1039/C9EE01935A.

[11] G.G. Zhang, Z.A. Lan, X.C. Wang, Conjugated polymers: catalysts for photocatalytic hydrogen evolution, Angew. Chem., Int. Ed. 55 (2016) 15712–15727, https://doi.org/10.1002/anie.201607375.

[12] T. Banerjee, F. Podjaski, J. Kröger, B.P. Biswal, B.V. Lotsch, Polymer photocatalysts for solar-to-chemical energy conversion, Nat. Rev. Mater. 6 (2021) 168–190, https://doi.org/10.1038/s41578-020-00254-z.

[13] J.S. Zhang, Y. Chen, X.C. Wang, Two-dimensional covalent carbon nitride nanosheets: synthesis, functionalization, and applications, Energy Environ. Sci. 8 (2015) 3092–3108, https://doi.org/10.1039/C5EE01895A.

[14] J. Liu, H.Q. Wang, M. Antonietti, Graphitic carbon nitride "reloaded'': emerging applications beyond (photo)catalysis, Chem. Soc. Rev. 45 (2016) 2308–2326, https://doi.org/10.1039/C5CS00767D.

[15] S.W. Cao, J.X. Low, J.G. Yu, M. Jaroniec, Polymeric photocatalysts based on graphitic carbon nitride, Adv. Mater. 27 (2015) 2150–2176, https://doi.org/10.1002/adma.201500033.

[16] S. Yanagida, A. Kabumoto, K. Mizumoto, C. Pac, K. Yoshino, Poly(p-phenylene)-catalysed photoreduction of water to hydrogen, J. Chem. Soc. Chem. Commun. 8 (1985) 474–475, https://doi.org/10.1039/C39850000474.

[17] J.L. Wang, G. Ouyang, Y. Wang, X.L. Qiao, W.S. Li, H.Q. Li, 1,3,5-Triazine and dibenzo[b,d]thiophene sulfone based conjugated porous polymers for highly efficient photocatalytic hydrogen evolution, Chem. Commun. 56 (2020) 1601–1604, https://doi.org/10.1039/C9CC08412F.

[18] J.-S.M. Lee, A.I. Cooper, Advances in conjugated microporous polymers, Chem. Rev. 120 (2020) 2171–2214, https://doi.org/10.1021/acs.chemrev.9b00399.

[19] S.H. Luo, Z.T. Zeng, H. Wang, W.P. Xiong, B. Song, C.Y. Zhou, A. Duan, X.F. Tan, Q. Y. He, G.M. Zeng, Z.F. Liu, R. Xiao, Recent progress in conjugated microporous polymers for clean energy: synthesis, modification, computer simulations, and applications, Prog. Polym. Sci. 115 (2021), 101374, https://doi.org/10.1016/j.progpolymsci.2021.101374.

[20] H. Wang, H. Wang, Z.W. Wang, L. Tang, G.M. Zeng, P. Xu, M. Chen, T. Xiong, C. Y. Zhou, X.Y. Li, D.L. Huang, Y. Zhu, Z.X. Wang, J.W. Tang, Covalent organic framework photocatalysts: structures and applications, Chem. Soc. Rev. 49 (2020) 4135–4165, https://doi.org/10.1039/D0CS00278J.

[21] Q. Yang, M.L. Luo, K.W. Liu, H.M. Cao, H.J. Yan, Covalent organic frameworks for photocatalytic applications, Appl. Catal. B Environ. 276 (2020), 119174, https://doi.org/10.1016/j.apcatb.2020.119174.

[22] C.L. Xia, K.O. Kirlikovali, T.H.C. Nguyen, X.C. Nguyen, Q.B. Tran, M.K. Duong, M. T.N. Dinh, D.L.T. Nguyen, P. Singh, P. Raizada, V.-H. Nguyen, S.Y. Kim, L. Singh, C. C. Nguyen, M. Shokouhimehr, Q.V. Le, The emerging covalent organic frameworks (COFs) for solar-driven fuels production, Coord. Chem. Rev. 446 (2021), 214117, https://doi.org/10.1016/j.ccr.2021.214117.

[23] S. Li, M.F. Wu, T. Guo, L.L. Zheng, D.K. Wang, Y. Mu, Q.J. Xing, J.P. Zou, Chlorine-mediated photocatalytic hydrogen production based on triazine covalent organic framework, Appl. Catal. B Environ. 272 (2020), 118989, https://doi.org/10.1016/j.apcatb.2020.118989.

[24] D. Kong, X.Y. Han, J.J. Xie, Q.S. Ruan, C.D. Windle, S. Gadipelli, K. Shen, Z.M. Bai, Z.X. Guo, J.W. Tang, Tunable covalent triazine-based frameworks (CTF-0) for visible-light-driven hydrogen and oxygen generation from water splitting, ACS Catal. 9 (2019) 7697–7707, https://doi.org/10.1021/acscatal.9b02195.

[25] V.S. Vyas, F. Haase, L. Stegbauer, G. Savasci, F. Podjaski, C. Ochsenfeld, B. V. Lotsch, A tunable azine covalent organic framework platform for visible light-induced hydrogen generation, Nat. Commun. 6 (2015) 8508, https://doi.org/10.1038/ncomms9508.

[26] T. Zhang, W.B. Lin, Metal-organic frameworks for artificial photosynthesis and photocatalysis, Chem. Soc. Rev. 43 (2014) 5982–5993, https://doi.org/10.1039/C4CS00103F.

[27] W. Wang, X.M. Xu, W. Zhou, Z.P. Shao, Recent progress in metal-organic frameworks for applications in electrocatalytic and photocatalytic water splitting, Adv. Sci. 4 (2017), 1600371, https://doi.org/10.1002/advs.201600371.

[28] Y.Y. Liu, B.J. Li, Z.H. Xiang, Pathways towards boosting solar-driven hydrogen evolution of conjugated polymers, Small 17 (2021), 2007576, https://doi.org/10.1002/smll.202007576.

[29] C.H. Dai, Y.T. Pan, B. Liu, Conjugated polymer nanomaterials for solar water splitting, Adv. Energy Mater. 10 (2020), 2002474, https://doi.org/10.1002/aenm.202002474.

[30] J.Z. Cheng, L.L. Liu, G.F. Liao, Z.Q. Shen, Z.R. Tan, Y.Q. Xing, X.X. Li, K. Yang, L. Chen, S.Y. Liu, Achieving an unprecedented hydrogen evolution rate by solvent-exfoliated CPP-based photocatalysts, J. Mater. Chem. A 8 (2020) 5890–5899, https://doi.org/10.1039/C9TA13514F.

[31] C. Shu, C.Z. Han, X.Y. Yang, C. Zhang, Y. Chen, S.J. Ren, F. Wang, F. Huang, J. X. Jiang, Boosting the photocatalytic hydrogen evolution activity for D–π–A conjugated microporous polymers by statistical copolymerization, Adv. Mater. 33 (2021), 2008498, https://doi.org/10.1002/adma.202008498.

[32] G. Shu, Y.D. Li, Z. Wang, J.X. Jiang, F. Wang, Poly(dibenzothiophene-S,S-dioxide) with visible light-induced hydrogen evolution rate up to 44.2 mmol h^{-1} g^{-1} promoted by K_2HPO_4, Appl. Catal. B Environ. 261 (2020), 118230, https://doi.org/10.1016/j.apcatb.2019.118230.

[33] Z.A. Lan, W. Ren, X. Chen, Y.F. Zhang, X.C. Wang, Conjugated donor-acceptor polymer photocatalysts with electron-output “tentacles” for efficient hydrogen evolution, Appl. Catal. B Environ. 245 (2019) 596–603, https://doi.org/10.1016/j.apcatb.2019.01.010.

[34] J.L. Wang, G. Ouyang, D.W. Wang, J. Li, J.H. Yao, W.S. Li, H.X. Li, Enhanced photocatalytic performance of donor-acceptor-type polymers based on a thiophene-contained polycyclic aromatic unit, Macromolecules 54 (2021) 2661–2666, https://doi.org/10.1021/acs.macromol.1c00316.

[35] W. Zhou, T. Jia, D.Q. Zhang, Z.K. Zheng, W. Hong, X.D. Chen, The enhanced co-catalyst free photocatalytic hydrogen evolution and stability based on indenofluorene-containing donor-acceptor conjugated polymer dots/g-C_3N_4 nanosheets heterojunction, Appl. Catal. B Environ. 259 (2019), 118067, https://doi.org/10.1016/j.apcatb.2019.118067.

[36] C.X. Lin, X.L. Liu, B.Q. Yu, C.Z. Han, L. Gong, C.M. Wang, Y. Gao, Y.Z. Bian, J. Z. Jiang, Rational modification of two-dimensional donor-acceptor covalent organic frameworks for enhanced visible light photocatalytic activity, ACS Appl. Mater. Interfaces 13 (2021) 27041–27048, https://doi.org/10.1021/acsami.1c04880.

[37] Q.Y. Wei, X.Q. Yao, Q.Q. Zhang, P.J. Yan, C.L. Ru, C.F. Li, C.L. Tao, W. Wang, D. F. Han, D.X. Han, L. Niu, D.D. Qin, X.B. Pan, Nanostructured lateral boryl substitution conjugated donor-acceptor oligomers for visible-light-driven hydrogen production, Small 17 (2021), 2100132, https://doi.org/10.1002/smll.202100132.

[38] P. Pachfule, A. Acharjya, J. Roeser, R.P. Sivasankaran, M.Y. Ye, A. Brückner, J. Schmidt, A. Thomas, Donor–acceptor covalent organic frameworks for visible light induced free radical polymerization, Chem. Sci. 10 (2019) 8316–8322, https://doi.org/10.1039/C9SC02601K.

[39] J. Yu, X.Q. Sun, X.X. Xu, C. Zhang, X.M. He, Donor–acceptor type triazine-based conjugated porous polymer for visible-light-driven photocatalytic hydrogen evolution, Appl. Catal. B Environ. 257 (2019), 117935, https://doi.org/10.1016/j.apcatb.2019.117935.

[40] W.Q. Li, X.F. Huang, T.W. Zeng, Y.H.A. Liu, W.B. Hu, H. Yang, Y.B. Zhang, K. Wen, Donor-acceptor covalent organic framework for sunlight-driven hydrogen evolution, Angew. Chem. Int. Ed. 60 (2021) 1869–1874, https://doi.org/10.1246/cl.200834.

[41] F.T. Yu, Z.Q. Wang, S.C. Zhang, W.J. Wu, H.N. Ye, H.R. Ding, X.Q. Gong, J.L. Hua, Construction of polymeric carbon nitride and dibenzothiophene dioxide-based intramolecular donor-acceptor conjugated copolymers for photocatalytic H_2 evolution, Nanoscale Adv. 3 (2021) 1699–1707, https://doi.org/10.1039/D0NA01011A.

[42] S. Fukuzumi, K. Ohkubo, T. Suenobu, Long-lived charge separation and applications in artificial photosynthesis, Acc. Chem. Res. 47 (2014) 1455–1464, https://doi.org/10.1021/ar400200u.

[43] W.R. Wang, J. Li, Q. Li, Z.W. Xu, L.N. Liu, X.Q. Chen, W.J. Xiao, J.H. Yao, F. Zhang, W.S. Li, Side-chain-extended conjugation: a strategy for improving the photocatalytic hydrogen production performance of a linear conjugated polymer, J. Mater. Chem. A 9 (2021) 8782–8791, https://doi.org/10.1039/D0TA12425G.

[44] X.Y. Wang, L.J. Chen, S.Y. Chong, M.A. Little, Y.Z. Wu, W.H. Zhu, R. Clowes, Y. Yan, M.A. Zwijnenburg, R.S. Sprick, A.I. Cooper, Sulfone-containing covalent organic frameworks for photocatalytic hydrogen evolution from water, Nat. Chem. 10 (2018) 1180–1189, https://doi.org/10.1038/s41557-018-0141-5.

[45] C.H. Dai, S.D. Xu, W. Liu, X.Z. Gong, M. Panahandeh-Fard, Z.T. Liu, D.Q. Zhang, C. Xue, K.P. Loh, B. Liu, Dibenzothiophene-S,S-dioxide-based conjugated polymers: highly efficient photocatalysts for hydrogen production from water under visible light, Small 14 (2018), 1801839, https://doi.org/10.1002/smll.201801839.

[46] C. Yang, B.C. Ma, L.Z. Zhang, S. Lin, S. Ghasimi, K. Landfester, K.A.I. Zhang, X. C. Wang, Molecular engineering of conjugated polybenzothiadiazoles for enhanced hydrogen production by photosynthesis, Angew. Chem. Int. Ed. 55 (2016) 9202–9206, https://doi.org/10.1002/ange.201603532.

[47] C. Cheng, X.C. Wang, Y.Y. Lin, L.Y. He, J.X. Jiang, Y.F. Xu, F. Wang, The effect of molecular structure and fluorination on the properties of pyrene-benzothiadiazole-based conjugated polymers for visible-light-driven hydrogen evolution, Polym. Chem. 9 (2018) 4468–4475, https://doi.org/10.1039/C8PY00722E.

[48] Y.B. Hu, Y.X. Liu, J. Wu, Y.D. Li, J.X. Jiang, F. Wang, A case study on a soluble dibenzothiophene-S,S-dioxide-based conjugated polyelectrolyte for photocatalytic hydrogen production: the film versus the bulk material, ACS Appl. Mater. Interfaces 13 (2021) 42753–42762, https://doi.org/10.1021/acsami.1c10748.

[49] G. Shu, Y. Wang, Y.D. Li, S. Zhang, J.X. Jiang, F. Wang, A high performance and low cost poly(dibenzothiophene-S,S-dioxide)@TiO_2 composite with hydrogen evolution rate up to 51.5 mmol $h^{-1}g^{-1}$, J. Mater. Chem. A 8 (2020) 18292–18301, https://doi.org/10.1039/D0TA06159J.

[50] C.M. Aitchison, R.S. Sprick, A.I. Cooper, Emulsion polymerization derived organic photocatalysts for improved light-driven hydrogen evolution, J. Mater. Chem. A 7 (2019) 2490–2496, https://doi.org/10.1039/C8TA11383A.

[51] M. Sachs, R.S. Sprick, D. Pearce, S.A.J. Hillman, A. Monti, A.A.Y. Guilbert, N. J. Brownbill, S. Dimitrov, X.Y. Shi, F. Blanc, M.A. Zwijnenburg, J. Nelson, J. R. Durrant, A.I. Cooper, Understanding structure-activity relationships in linear polymer photocatalysts for hydrogen evolution, Nat. Commun. 9 (2018) 4968, https://doi.org/10.1038/s41467-018-07420-6.

[52] D.F. Xu, B. Cheng, S.W. Cao, J.G. Yu, Enhanced photocatalytic activity and stability of Z-scheme Ag_2CrO_4-GO composite photocatalysts for organic pollutant degradation, Appl. Catal. B Environ. 164 (2015) 380–388, https://doi.org/10.1016/j.apcatb.2014.09.051.

[53] H. Chai, L.L. Gao, P. Wang, F. Li, G.W. Hu, J. J, In_2S_3/F-Fe_2O_3 type-II heterojunction bonded by interfacial S-O for enhanced charge separation and

transport in photoelectrochemical water oxidation, Appl. Catal. B Environ. 305 (2021), 121011, https://doi.org/10.1016/j.apcatb.2021.121011.

[54] J. Kosco, M. Sachs, R. Godin, M. Kirkus, L. Francas, M. Bidwell, M. Qureshi, D. Anjum, J.R. Durrant, I. Mcculloch, The effect of residual palladium catalyst contamination on the photocatalytic hydrogen evolution activity of conjugated polymers, Adv. Energy Mater. 8 (2018), 1802181, https://doi.org/10.1002/aenm.201802181.

[55] C.M. Li, H.H. Wu, D.Q. Zhu, T.X. Zhou, M. Yan, G. Chen, J.X. Sun, G. Dai, F. Ge, H. J. Dong, High-efficient charge separation driven directionally by pyridine rings grafted on carbon nitride edge for boosting photocatalytic hydrogen evolution, Appl. Catal. B Environ. 297 (2021), 120433, https://doi.org/10.1016/j.apcatb.2021.120433.